US Army Corps
of Engineers
Construction Engineering
Research Laboratories

USACERL Technical Report 97/119
July 1997

CONSTRUCTION PRODUCTIVITY ADVANCEMENT RESEARCH (CPAR) PROGRAM

Demonstration of Fiber-Reinforced Plastic Composite Rebar on a Full-Scale Concrete Bridge Deck

by

Jonathan C. Trovillion, Hota V.S. GangaRao, Sanjeev V. Kumar,
Hemanth K. Thippeswamy, and Lena Yoe

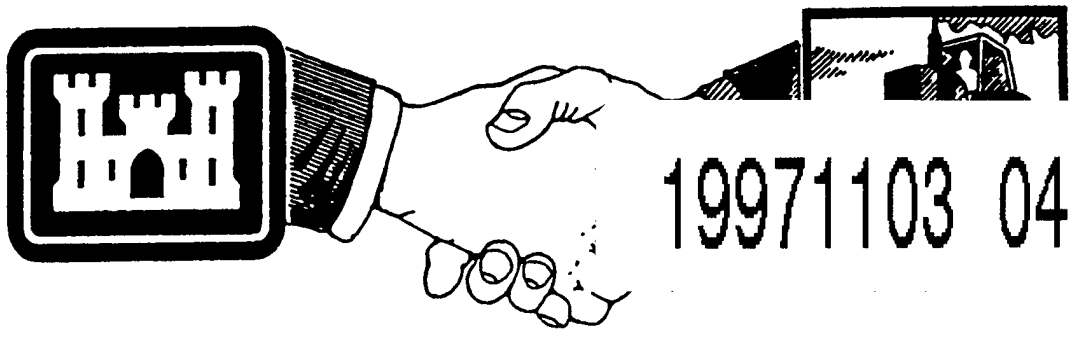

**A Corps/Industry Partnership To Advance
Construction Productivity and Reduce Costs**

REPORT DOCUMENTATION PAGE

Form Approved
OMB No. 0704-0188

1. AGENCY USE ONLY *(Leave Blank)*	2. REPORT DATE	3. REPORT TYPE AND DATES COVERED
	July 1997	Final

4. TITLE AND SUBTITLE
Demonstration of Fiber-Reinforced Plastic Composite Rebar on a Full-Scale Concrete Bridge Deck

5. FUNDING NUMBERS
CPAR
FAD 1-002443,
dated 27 September 1989

6. AUTHOR(S)
Jonathan C. Trovillion, Hota V.S. GangaRao, Sanjeev V. Kumar, Hemanth K. Thippeswamy, and Lena Yoe

7. PERFORMING ORGANIZATION NAME(S) AND ADDRESS(ES)
U.S. Army Construction Engineering Research Laboratories (USACERL)
P.O. Box 9005
Champaign, IL 61826-9005

8. PERFORMING ORGANIZATION REPORT NUMBER
TR 97/119

9. SPONSORING / MONITORING AGENCY NAME(S) AND ADDRESS(ES)
Headquarters, U.S. Army Corps of Engineers
ATTN: CEMP-CE
20 Massachusetts Ave. NW
Washington, DC 20314-1000

10. SPONSORING / MONITORING AGENCY REPORT NUMBER

11. SUPPLEMENTARY NOTES
Copies are available from the National Technical Information Service, 5285 Port Royal Road, Springfield, VA 22161.

12a. DISTRIBUTION / AVAILABILITY STATEMENT
Approved for public release; distribution is unlimited.

12b. DISTRIBUTION CODE

13. ABSTRACT (Maximum 200 words)
This report describes work conducted as part of a Construction Productivity Advancement Research (CPAR) project intended to demonstrate the effectiveness of fiber-reinforced plastic (FRP) reinforcement bars used in a full-scale bridge deck. The main benefit of FRP over mild steel reinforcement is its resistance to corrosive environments, which could significantly extend the service life of various reinforced concrete structures. A bridge needing replacement was identified near McKinleyville, WV, and the replacement was designed and constructed using FRP rebar instead of steel. This report describes the design methodologies necessary for utilizing FRP rebars in concrete reinforcement, and uses the actual replacement McKinleyville bridge deck design as an example. Also included are descriptions of activities by various research and standards organizations working to develop material specifications and design criteria for using FRP rebars as concrete reinforcement.

14. SUBJECT TERMS
Construction Productivity Advancement Research (CPAR) bridges
fiber-reinforced concrete
rebars

15. NUMBER OF PAGES
52

16. PRICE CODE

17. SECURITY CLASSIFICATION OF REPORT	18. SECURITY CLASSIFICATION OF THIS PAGE	19. SECURITY CLASSIFICATION OF ABSTRACT	20. LIMITATION OF ABSTRACT
Unclassified	Unclassified	Unclassified	SAR

Foreword

This study was conducted for Headquarters, U.S. Army Corps of Engineers under the Construction Productivity Advancement Research (CPAR) Work Unit "Development and Demonstration of a Full-Scale Concrete Bridge Deck Reinforced With Fiber-Reinforced Plastic (FRP)"; Funding Authorization Document (FAD) 1-002443, dated 27 September 1989. The technical monitors were Paul Tan, CECW-ED, D. Chen, CEMP-ET, and S. Green, CEMP-CE.

The work was executed through a CPAR Cooperative Research and Development Agreement between the Materials Science and Technologies Division (FL-M) of the Facilities Technology Laboratory (FL), U.S. Army Construction Engineering Research Laboratories (USACERL) and West Virginia University–Constructed Facilities Center (WVU–CFC). The USACERL Principal Investigator was Jonathan C. Trovillion, CECER-FL-M, and the WVU–CFC Principal Investigator was Dr. Hota V.S. GangaRao. International Grating, Inc. (Houston, TX), and Marshall Industries (Lima, OH) are acknowledged for providing fiber-reinforced plastic composite rebars as part of in-kind support for this CPAR demonstration. Special acknowledgment is given to Joe Darnell, Jennifer Fox, John Brunell, Dan Martin, and Jim Keffer of the West Virginia Department of Transportation–Division of Highways for their help and support during this project. Special thanks to Mark Steven "Steve" Peterson of the U.S. Army Corps of Engineers, Huntington District, for review and comment on the bridge deck design. Thanks also to Derek Altizer at West Virginia University for assistance testing FRP rebars. Dr. Ilker R. Adiguzel is Acting Chief, CECER-FL-M, and Donald R. Fournier is Acting Operations Chief, CECER-FL. The USACERL technical editor was Gordon L. Cohen, Technical Information Team.

Dr. Michael J. O'Connor is the Director of USACERL.

Contents

List of Figures

Figures

1 Introduction

Background

Corrosion-related deterioration of civil engineering structures over the past two decades has created an increasing need for costly repairs, and these repairs inevitably cause substantial user inconveniences while they are being done. Steel has traditionally been the material of choice for the reinforcement of concrete, but steel is not always the best choice in all applications. There is considerable interest in the idea of using fiber-reinforced plastic (FRP) reinforcement bars in place of the mild steel bars currently used for concrete reinforcement, especially in areas where corrosion resistance is required. The use of FRP reinforcement bars, or *rebars*, in bridge deck construction will have a major impact on selecting construction materials. FRP rebars are lightweight, durable, noncorrosive, and magnetically inert. FRP rebars resist the damaging effects of chemical deicing agents (salts) and they perform very well in other highly corrosive environments. Therefore, this material has the potential to significantly improve the longevity of structures such as bridge decks and parking garages. The successful demonstration of FRP rebars in structures such as concrete bridge decks—and the related field data to be collected—would provide the U.S. construction industry valuable, real-world technical information for incorporation into future designs.

Advanced materials such as FRP rebar are also greatly needed for the U.S. Army Corps of Engineers to accomplish its mission in repairing and replacing the Civil Works infrastructure for which it is responsible. The construction and monitoring of an FRP-reinforced concrete bridge deck is a necessary step if the Corps is to successfully adopt this technology.

Under the Corps of Engineers Construction Productivity Advancement Research (CPAR) program, a Cooperative Research and Development Agreement was initiated to demonstrate the application of FRP composite rebars in a full-scale bridge deck. The Corps partner laboratory was the U.S. Army Construction Engineering Research Laboratories (USACERL) and the industry partner was the Constructed Facilities Center at West Virginia University, Morgantown, WV. This CPAR demonstration was conducted in cooperation with the West Virginia Department of Transportation–Division of Highways.

Objective

The objective of this project was to demonstrate the advantages of specially designed FRP composite rebars to improve construction productivity and the long-term system durability (i.e., corrosion resistance) of reinforced concrete bridge decks. Material specifications, design, and construction standards will be developed for the use of FRP composite rebars.

Approach

This project was organized into two phases:

Phase I

- site selection
- design and analysis of bridge deck
- construction of bridge deck

Phase II

- performance monitoring, data collection, and analysis of data
- development of standards, specifications, and commercialization plan

Units of Weight and Measure

U.S. standard units of weight and measure are used in this report. A table of conversion factors for standard international (SI) units is presented below.

SI conversion factors

1 in.	=	25.4 mm
1 ft	=	0.305 m
1 lb	=	0.453 kg
1 gal	=	3.78 L
1 psi	=	6.89 kPa
°F	=	(°C × 1.8) +32

Symbols and Notation Used in This Report

The body of this report includes many formulas and calculations extracted from or based on standard engineering reference texts. A summary list of the symbols and notation used is provided below.

a = depth of equivalent rectangular stress block
A_b = area of rebars (in^2)
A_{FRP} = area of FRP rebars in tension (in^2)
$A_{FRP\ top}$ = area of FRP reinforcement on top section
$A_{FRP\ bottom}$ = area of FRP reinforcement on bottom section
$A_{FRP\ required}$ = area of FRP reinforcement required
A_c = effective tension area of concrete surrounding principal reinforcement divided by number of rebars (in^2)
A_s = cross sectional area of steel stringer
b = width of compression face of member
b_f = flange width of steel stringer
c = distance from extreme compression fiber to cracked neutral axis
c_{bal} = distance from extreme compression fiber to cracked neutral axis of balanced section
C = compressive force
d = distance from extreme compressive fiber to centroid of tension reinforcement
d_b = diameter of rebar (in)
d_c = effective concrete depth
d_s = diameter of shear stud connectors
D = diameter of reinforcement (in)
E_c = modulus of elasticity of concrete (psi)
E_f = modulus of elasticity of FRP rebars (ksi)
E_{FRP} = modulus of elasticity of FRP reinforcement (psi)
E_{reinf} = modulus of elasticity of reinforcement (psi)
E_s = modulus of elasticity of steel (psi)
f'_c = compressive strength of concrete (psi)
f'_t = tensile strength of concrete (psi)
f_c = stress in concrete (psi)
f_f = stress in FRP reinforcement (psi)
f_r = modulus of rupture of concrete (psi)
f_s = maximum stress reinforcement at service load (ksi)
f_{ss} = strenght of shear stud connectors
f_y = effective yield strenght of FRP rebars (psi)
I = crack spacing

I_a = impact allowance
I_{cr} = moment of inertia of cracked concrete section about centroidal axis
I_e = effective moment of inertia
I_g = moment of inertia of gross concrete section about centroidal axis
I_m = modified moment of inertia
jd = distance between the compressive and tensile force
k = proportionate multiplier of the depth
k_{bal} = proportionate multiplier of the depth for balanced section
kd = distance from extreme compression fiber to neutral axis
l = span length after continuity factor
l_d = embedment length (in.)
l_{db} = development length
L = span length
M = moment force
M_a = applied moment
M_{cr} = cracked moment
M_{curb} = moment due to curb
M_{DL} = moment due to dead load
$M_{factored}$ = factored total moment
M_{LL} = moment due to live load
$M_{overhang}$ = moment due to curb and overhang slab
M_{slab} = moment due to slab
M_T = unfactored total moment
M_u = ultimate moment
n = modular ratio of elasticity
N = number of shear studs
P = concentrated point load
P_1 = force on slab
P_2 = force on slab
P_{20} = HS 20 truck load
P_{25} = HS 25 truck load
Q = static moment about neutral axis
s = spacing between steel stringers
S = spacing between shear stud connectors
S_r = shear force per inch
S_u = allowable load per stud
t_s = depth of concrete section
T = tensile force
V_r = live load shear
W = uniformly distributed load
W_c = weight of concrete (psf)

W_{DL} = uniform dead load
W_{max} = maximum flexural crack width
W_s = weight of wearing surface (psf)
y = distance from centroidal axis of gross section to extreme fiber in tension
z = equivalent gross moment of inertia over distance y
Z_r = load range per shear connector
α = load cycles
β = ratio of distance to neutral axis from extreme tension fiber and centroid of main reinforcement
β_1 = multiplying factor dependent on the strength of concrete
Δ = deflection
Δ_{max} = maximum deflection
μ = bond strength (psi)
μ_m = maximum bond stress (psi)
ρ = ratio of nonprestressed tension reinforcement
ρ_{bal} = ratio of nonprestressed tension reinforcement for balanced section
ρ_{max} = maximum reinforcement ratio
ρ_{min} = minimum reinforcement ratio
$\rho_{provided}$ = amount of reinforcement provided
σ = stress at extreme fiber ends
ϕ = strength reduction factor

2 Site Selection and Replacement Bridge Design

The Original McKinleyville Bridge

The site for this CPAR project is the McKinleyville bridge, spanning Buffalo Creek in Brooke County, WV. The West Virginia Department of Transportation–Division of Highways (WVDOT–DOH) selected this bridge because it was already classified as structurally deficient and functionally obsolete. The site was determined by WDOT–DOH and the Constructed Facilities Center (CFC) of West Virginia University to be suitable for demonstration of a bridge deck reinforced with FRP composite rebar.

Built in 1915, the McKinleyville bridge was designed for lighter loads, lower traffic volumes, and slower driving speeds than typical of current usage patterns (Figure 1). The effects of aging plus various environmental factors accelerated the deterioration of the bridge. The original bridge was a rectangular, single-span Pratt truss bridge with an open steel grid deck supported on six steel stringers spaced at

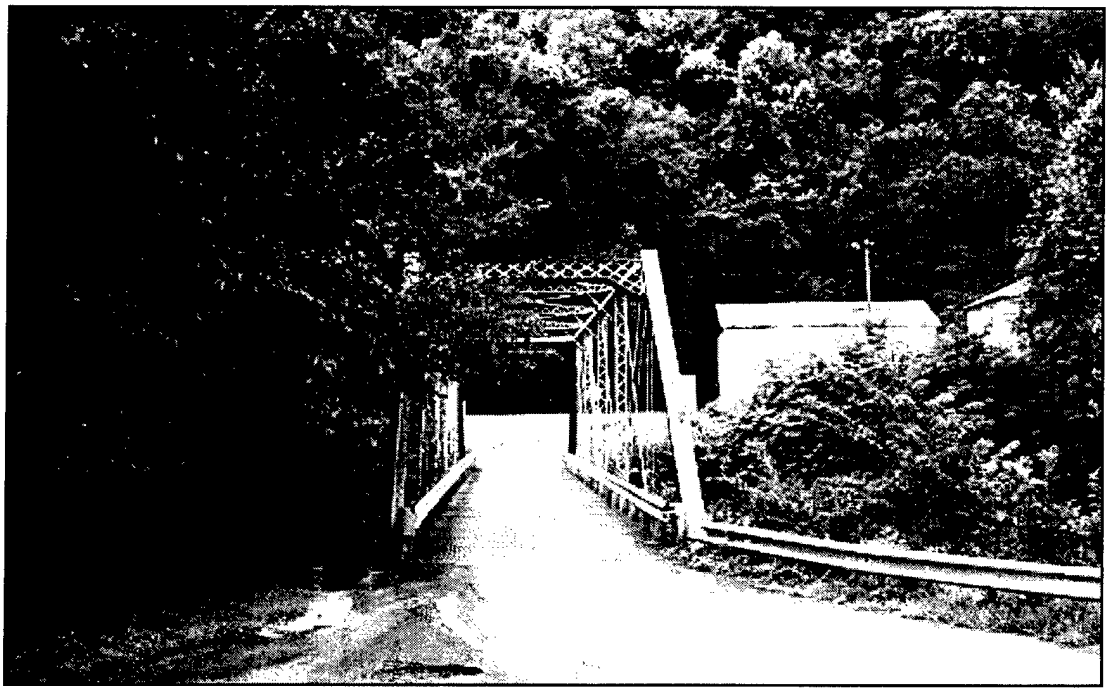

Figure 1. The original McKinleyville Bridge.

2 ft-6 in center to center (c/c). The deck was 109 ft-3 in long by 13 ft-3 in wide. The abutments and wingwalls were built of cut stone and the abutment seats were made of reinforced concrete. Two Pratt trusses were provided along both sides of the bridge, with a vertical clearance limit of 15 ft-1 in. The original design load and average daily traffic (ADT) are not known. The ADT values were 650 and 400 in 1990 and 1994, respectively.

Over the years, the bridge had undergone several rehabilitations. Before replacement, it was used as a single-lane structure with a posted maximum load limit of 12 tons. Recent bridge inspections determined that the bridge was in poor condition. All components, including railings and approach slabs, needed repair or replacement.

Replacement McKinleyville Bridge Design

The replacement bridge system consists of a rectangular, three-span bridge with a reinforced concrete deck stiffened with steel girders. The concrete deck is reinforced with fiber-reinforced plastic (FRP) rebars. The replacement design originally specified only sand-coated deformed FRP from International Grating, Inc. (Houston, TX). However, at a later stage the design was modified to include a non-coated deformed type of FRP rebar from Marshall Industries (Lima, OH). International Grating and Marshall Industries both provided the rebars at no cost. Both types are considered approximately equivalent in terms of shear transfer from concrete to bar, so both were specified in this demonstration to determine whether any differences would show up after longer-term monitoring in service. (Chapter 4 discusses some slight deck design modifications made necesary due to the limited selection of non-coated rebar grades that were commercially available at the time.)

The replacement bridge accommodates two lanes, with a total span of 177 ft in three sections (52 ft, 72 ft, and 52 ft) and a total width of 29.5 ft. The concrete slab thickness is taken to be 9 in., and each of the six steel stringers are spaced at 5 ft.

The cross-section of the bridge is obtained from considering an equivalent simply supported bridge and by satisfying the strength and serviceability requirements. The bridge is analyzed as a composite as well as a non-composite section. The primary loads considered are *dead load*, *live load*, and *braking load*. The secondary loads considered are *dead load plus creep* of the material, *temperature gradient* across the bridge depth, *uniform shrinkage of the concrete* in the bridge deck, and *differential settlement* of the supports. The bridge design parameters are summarized as follows:

- Bridge spans: 3 spans—52 ft, 72 ft, and 52 ft
- No. of lanes: 2
- No. of stringers: 6
- Stringer size: WF 33 x 130
- Stringer steel grade: 50
- Abutment type: Integral
- Abutment foundation: Single row of piles 40 ft long, with weak axis bending
- Slab overhang: 2 ft - 3 in. beyond centerline of extreme stringers
- Top clear cover for slab: 1.5 in.
- Bottom clear cover for slab: 1 in.
- FRP type: Sand-coated, deformed (later modified to include non-coated, deformed)
- FRP ultimate strength (#3 bars): 100 ksi
- Average concrete compressive strength: 4500 psi

Design of Superstructure Abutment Joint

The abutment and deck are cast integrally, with conventional steel reinforcement tying the two structures at the joint. The foundation of the abutment consists of a single row of piles oriented such that the weak axis is perpendicular to the flow of traffic. The abutment accommodates the embedded piles. The approach slab rests on a concrete seat provided in the abutment.

Design of Superstructure Pier Joint

The bottom flange of each stringer is welded to a sole plate, which rests on an elastomeric bearing pad. The elastomeric bearing pad rests on a second sole plate, which is integral with the pier cap. The top and bottom sole plates are further connected by means of bolts. Because this is a jointless bridge, holes in the top sole plate are made larger than the size of the bolts to provide for movement of the bridge under thermal expansion and contraction. This arrangement ensures free movement of the superstructure as well as the transfer of shear forces only from superstructure to pier. The bolts and sole plates are specified to be stainless steel for corrosion resistance.

Pavement, Approach Slab, and Abutment Joints

The cycle control joint and the pressure relief joint are each filled with sealants. A shear type connection is to be used between the approach slab and the abutment. A sleeper slab provides a solid base for the approach slab and pavement ends. A filter fabric underneath the approach slab ensures proper horizontal movement of

the approach slab. A fully stabilized backfill can prevent settlement and erosion, while a drainage system can provide for proper functioning of the approach slab and backfill.

3 Design Methodolgies for FRP Composites

Background

Through externally sponsored research from different agencies, before this CPAR project, CFC had conducted a multiyear study to evaluate the behavior of FRP rebars and their use in concrete structures, as well as the behavior of concrete beams and decks reinforced with FRP rebars. That study produced basic engineering performance criteria and composition improvements of the composite rebar. The design methodologies presented in this report take advantage of their research and experience in this area. A description of this work is given in a CFC report entilted, "Bending and Bond Behavior and Design of Concrete Beams Reinforced with Fiber Reinforced Plastic Rebars."

Design of Concrete Beams Reinforced with FRP Rebars

The performance of FRP rebars in concrete is not fully known although they have been used in structural applications. The properties of the material—high strength, noncorrosive, nonmagnetic, and lightweight—should allow for greater leeway in the design requirements. However, the current mathematical models and design equations used for mild steel cannot be directly applied to beams reinforced with FRP for the following reasons:

1. Glass FRP rebars have a low modulus of elasticity compared to mild steel.
2. FRP rebars have greater long-term corrosion-resistance than mild steel.
3. The bond behavior of FRP rebars is not yet well understood.
4. Crack width development and post-cracking behavior of concrete beams reinforced with FRP rebars differs from conventional reinforced beams.

In order to develop a design methodology for concrete beams reinforced with FRP rebars, theoretical correlations with experimental results are conducted in terms of elastic and ultimate bending moment, crack width, post-cracking deflection, development length, and bond length. Simple design equations, parallel to the ACI (American Concrete Institute) 318-89 code, have been developed for concrete beams reinforced with FRP rebars for both the working stress and the ultimate design

method (GangaRao and Faza 1992). These design equations are established using the balanced reinforcement approach so FRP reinforced concrete beam design can parallel that of steel reinforced beams. The equations apply to FRP rebars composed of thermoset resins, vinyl ester or isophthalic, and continuous E-glass fibers. Because the modified equations are dependent on material type, other fibers and resins require modification in the values of modulus of elasticity and ultimate strength before the equations can be applied.

In the ultimate strength design method for steel, design is based upon the ultimate compressive strength and strain of concrete and the yield strength of the reinforcement. The effective pseudo-yield strength (no significant yielding) of FRP rebars depends upon the diameter of the bar. This value ranges from 104 ksi for a #3 rebar to 64 ksi for a #8 rebar (GangaRao and Faza 1992, p 156). This decrease in ultimate tensile strength with increasing diameter is due to the dependence of resin on the shear lag phenomenon. Ultimate strength also varies with manufacture configuration, such as fibers that are unidirectional versus braided, or wrapped versus unwrapped. The yield strength is taken to be equivalent to the effective yield strength (at a 2 percent offset) by use of a reduction factor to account for manufacturing variations as well as the FRP rebars not exhibiting a yield plateau.

In the working stress method, the allowable design stress for the rebars is taken as a percentage of the ultimate yield strength. For FRP rebars, this value is half of the effective yield strength. This value is acceptable for beams under nonsustaining loads. A value of one-quarter the effective yield strength should be used for sustaining load cases, which accounts for the premature cracking of the beam.

Ultimate Moment Capacity

Ultimate Strength Method

The compressive stress distribution in concrete beams subjected to bending is directly related to the shape of the stress-strain curve. Due to differences in the shape of the stress-strain curve of high-strength concrete and the low modulus of elasticity of the FRP rebar (which causes the neutral axis to shift closer towards the compression fiber), the compressive stress distribution of concrete reinforced with FRP rebars is expected to be different from that of the steel rebars.

Investigation of the calculated ultimate moment capacity based upon a rectangular stress distribution and that of a parabolic distribution concluded that there is negligible difference between the two (GangaRao and Faza 1992, p 101). Thus, it

is accurate to assume a rectangular stress distribution for concrete reinforced with both steel and FRP rebars. The ultimate moment capacity is obtained by satisfying internal forces and moment equilibrium equations.

Figure 2 shows the Whitney block from which the ultimate strength design equations are derived. ACI 10.2.7.1 assumes a concrete stress of 0.85 f'_c over the equivalent compression zone. The distance "a" is the depth of the equivalent stress block. It is related to "c", the distance between the outside compression surface and the neutral axis by a multiplier β_1. The depth "d" is the distance from the compression surface to the centroid of the tension steel. The variable "jd" is the distance between the compressive and tensile force. The ultimate resisting moment (M_u) is given in ACI 9.1.2 as:

$$M_u = A_{FRP} f_y jd$$
$$= A_{FRP} f_y (d - \frac{a}{2}) \qquad \text{[Eq 1]}$$

where A_{FRP} = area of FRP rebars in tension (in^2)
f_y = effective yield strength of FRP rebars (psi)

This expression is independent of whether steel or FRP reinforcement is used because the development of moment resistance is the same in either section. The respective reinforcement area and yield strength should be applied depending on the type of reinforcement used. In order to obtain full bending resistance of the section, failure from bond, shear, and compression must be avoided.

To take advantage of the high tensile strength of the FRP rebars, high-strength concrete should be used to maximize bending resistance. High strength concrete also increases the cracking moment capacity of the beam, as well as decreasing the resulting crack width.

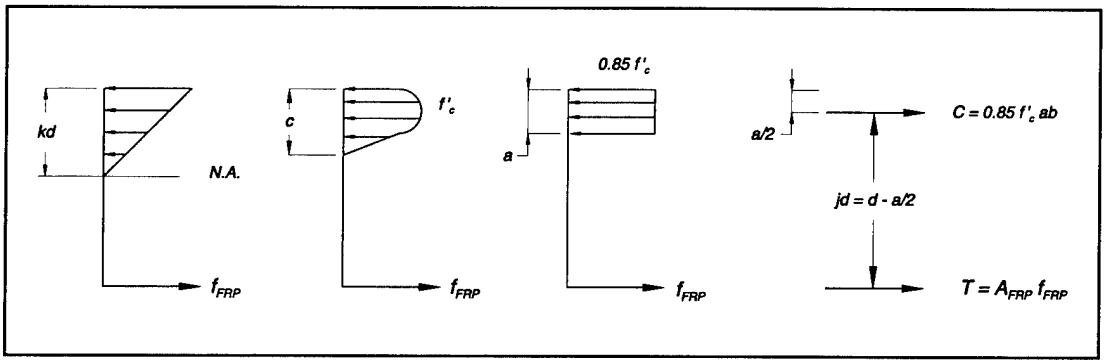

Figure 2. Whitney block equivalent.

Working Stress Method

The ultimate moment capacity in the working stress method can be determined in the same way. Figure 3 shows the flexural stresses and strains produced by service-load moments that are used in formulating the equations for the working stress method. These equations are given in CFC-92-142, section 6.1 (GangaRao and Faza 1992). "kd" represents the distance from the top surface to the neutral axis, where "k" is a proportionate multiplier of the depth. The CFC-92-142 equations (6-17) and (6-18) give the formulas for "k" and "k_{bal}". Equations (6-20) and (6-21) state that there are two controlling capacities. The first is obtained by summing moments about the compressive force while the second is obtained by summing forces about the tensile force. The width "b" is taken to be a 1 ft span.

$k < k_{bal}$: reinforcement stress controls design

$$M_u = A_{FRP} f_y jd = A_{FRP} f_y d(1 - \frac{k}{3}) \quad \text{[Eq 2]}$$

$k > k_{bal}$: concrete stress controls design

$$M_u = \frac{1}{2} f'_c bkjd^2 = \frac{1}{2} f'_c bkd^2(1 - \frac{k}{3}) \quad \text{[Eq 3]}$$

where

$$k = \sqrt{\rho^2 n^2) + 2\rho n} - \rho n$$
$$k_{bal} = \frac{nf'_c}{nf'_c + f_f} \quad \text{[Eq 4]}$$

The modular ratio "n" is given in ACI A.5.4 to convert between equivalent reinforcement and concrete sections. The formula provided for this ratio is:

$$n = \frac{E_{reinf}}{E_c} \quad \text{[Eq 5]}$$

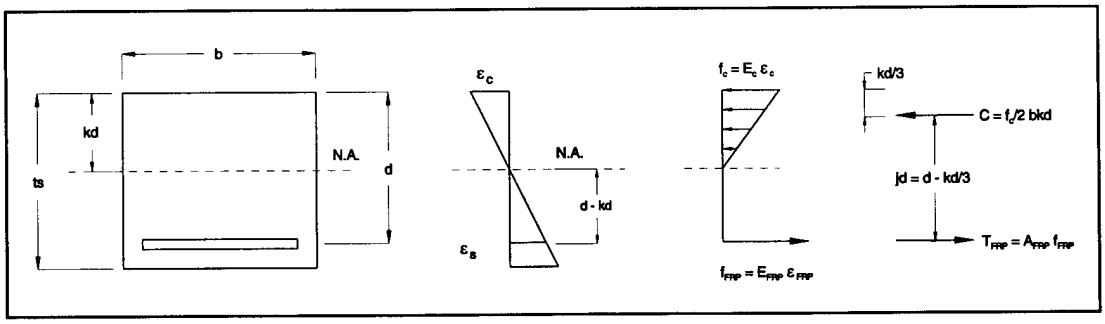

Figure 3. Flexural stresses and strains.

Flexural Cracking

A limit is placed on excessive cracking of a concrete section because cracking leads to reduction in stiffness, increase in deterioration problems, and it is aesthetically unpleasing. ACI places a limit on acceptable crack width to ensure that this distress takes the form of many fine cracks as opposed to fewer large ones. This limit is less a problem for FRP rebars than for steel rebars, although some sort of long-term degradation will take place.

Crack width is dependent on the reinforcement stress, thickness of concrete cover, area of concrete surrounding the rebar, and the stress gradient from the reinforcement to the tension face. Cracking is expected to occur when the induced tensile stress in the beam reaches the ultimate concrete tensile stress. The tensile stress is then transferred to the reinforcing bars through bond forces developed between the rebar and the concrete. The maximum flexural crack width (W_{max}) can be measured according to the Gergley-Lutz expression for steel-reinforced concrete given in ACI 10.6.4:

$$W_{max} = 0.076 \beta f_s \sqrt[3]{d_c A} \times 10^{-3} \quad \text{[Eq 6]}$$

where f_s = maximum stress (ksi) in reinforcement at service load
β = ratio of distance to neutral axis from extreme tension fiber and from the centroid of the main reinforcement

A value of 1.2 is used to estimate the crack widths obtained in flexure.

This equation must be modified when applied to concrete with FRP rebars. The strains in FRP rebars are expected to be four times as great as those of steel reinforcement because the modulus of elasticity is 7.2×10^6 psi, compared to 29×10^6 psi for steel. By incorporating FRP properties and substituting, the Gergley-Lutz expression for crack width is expressed as:

$$W_{max} = 0.3 \beta f_f \sqrt[3]{d_c A} \times 10^{-3} \quad \text{[Eq 7]}$$

where f_f = FRP stress (ksi)

This equation is valid only with the assumption that the same crack spacing occurs when using FRP rebars in place of steel rebars. Because crack spacing is governed by the tensile strength of concrete and the bond strength of the rebar, a relationship is developed between the tensile strength of concrete, bond strength, and crack spacing. Assuming bond strength is constant upon reaching the ultimate strength

of concrete, the crack spacing (I) defined by Watstein and Bresler (1972) is given in CFC-92-142 equation (5-10) as:

$$l = \frac{2 f'_t A_c}{\mu_m \pi D} \quad \text{[Eq 8]}$$

where f'_t = tensile strength of concrete (psi)
μ_m = maximum bond stress (psi)
D = diameter of rebar (in.)
A_c = effective tension area of concrete surrounding the principal reinforcement divided by the number of rebars (sq in.)

Substituting this expression into the Gergley-Lutz equation produces a final result, as given in CFC-92-142 equation (5-13), of:

$$W_{max} = \frac{f_f}{E_f} l = 0.14 f_f \frac{2 f'_t}{\mu_m} \frac{A_c}{\pi D} x\ 10^{-3} \quad \text{[Eq 9]}$$

where E_f = modulus of elasticity of FRP rebar (ksi)

Deflection

To satisfy deflection limits, maximum deflection of the FRP reinforced concrete beams under service loads is determined using either the gross moment of inertia (pre-cracking stage) or the effective moment of inertia (post-cracking stage). In the pre-cracking stage, deflection is controlled by a fully elastic behavior. The gross moment of inertia (I_g) is found by:

$$I_g = \frac{b t_s^3}{12} \quad \text{[Eq 10]}$$

In the post-cracking stage, the contribution of concrete in tension is negligible. The stiffness continues to decrease with increasing load until it reaches a lower limit that corresponds to the cracked moment of inertia (I_{cr}). This value can be obtained by taking the moment of inertia of the cracked section about the neutral axis after neglecting the concrete section in tension. It is given in CFC-92-142, equation (5-16) as:

$$I_{cr} = \frac{b c^3}{3} + n A_{FRP} (d - c)^2 \quad \text{[Eq 11]}$$

where c = distance from top fiber to the cracked neutral axis

In actual cases, only a portion of the beam is cracked, while the uncracked sections below the neutral axis still possess some degree of stiffness. An equivalent moment of inertia (I_e) provided in ACI 9.5.2.3 gives this value to be:

$$I_e = I_{cr} + \left(\frac{M_{cr}}{M_a}\right)^3 (I_g - I_{cr}) \qquad \text{[Eq 12]}$$

where M_{cr} = cracked moment
M_a = applied moment

Since crack pattern significantly influences the moment of inertia value, a modified moment of inertia (I_m) concept is introduced to replace the effective moment of inertia defined in ACI documentation. This expression is based on the assumption that the concrete section between the point loads is fully cracked, while the end sections are partially cracked. For the case of two concentrated point loads (P) applied at a third point over the length of the beam (L), the modified moment of inertia and deflection (Δ) are given in CFC-92-142, section 5.3.2.1, as:

$$I_m = \frac{23\, I_{cr} I_e}{8\, I_{cr} + 15\, I_e}$$
$$\Delta_{max} = \frac{23\, P L^3}{648\, E_c I_m} \quad (inches) \qquad \text{[Eq 13]}$$

For the case of a concentrated point load applied at the center of the beam, the expressions are:

$$I_m = \frac{54\, I_{cr} I_e}{23\, I_{cr} + 45\, I_e}$$
$$\Delta_{max} = \frac{P L^3}{48\, E_c I_m} \quad (inches) \qquad \text{[Eq 14]}$$

For the case of a uniform distributed load (W) applied to the beam, the expressions are:

$$I_m = \frac{240\, I_{cr} I_e}{39\, I_{cr} + 201\, I_e}$$
$$\Delta_{max} = \frac{5\, W L^4}{384\, E_c I_m} \quad (inches) \qquad \text{[Eq 15]}$$

Balanced Reinforcement Ratio

The balanced reinforcement ratio is a function of concrete strength, modulus of elasticity, and effective yield strength of FRP rebars, irrespective of section geometry. This assessment for concrete reinforced with FRP rebars is similar to the ACI ultimate design method for steel reinforcement.

Using the linear strain distribution diagram for balanced strain conditions shown in Figure 4, the c/d ratio for steel reinforcement is given as:

$$\frac{c_{bal}}{d} = \frac{0.003}{0.003 + \frac{f_y}{E_s}} \qquad \text{[Eq 16]}$$

Substituting E_{FRP} for E_s and the yield strength of FRP reinforcement results in a modified equation for FRP reinforced sections:

$$\frac{c_{bal}}{d} = \frac{19500}{19500 + f_y} \qquad \text{[Eq 17]}$$

The equivalent depth "a" of the rectangular stress block is obtained from the balanced stress block shown in Figure 2. Values for β_1 is given in ACI 10.2.7.3.

$$a = \frac{A_{FRP} f_y}{0.85 f'_c b} = \beta_1 c_{bal} \qquad \text{[Eq 18]}$$

Equating the above two expressions and using $\rho = A_{FRP}/bd$ give the reinforcement

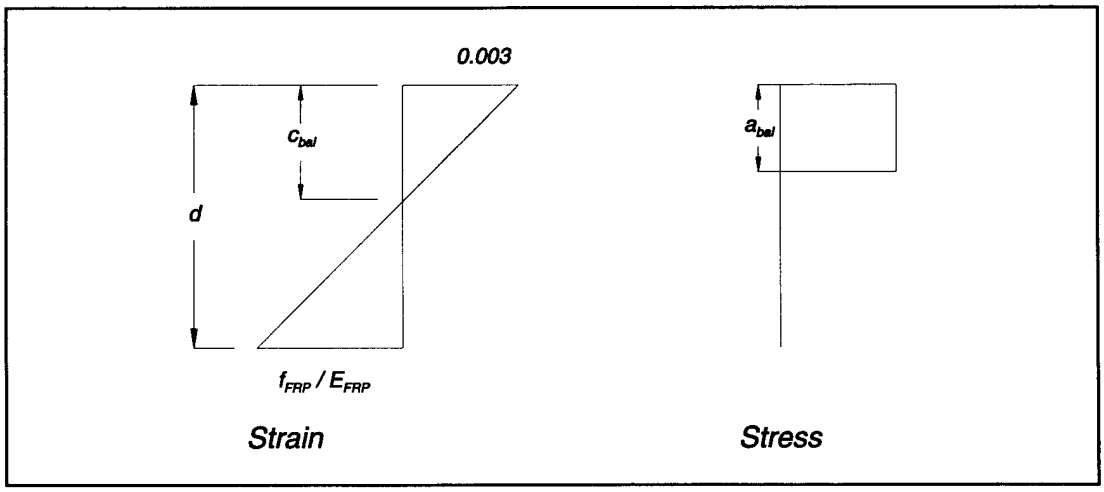

Figure 4. Strain and stress distribution diagram.

ratio for the balanced section (ρ_{bal}). This is equation (5-33) in CFC-92-142 (f_y and f'_c in psi):

$$\rho_{bal} = \frac{0.85 f'_c \beta_1}{f_y} \frac{19500}{19500 + f_y} \quad \text{[Eq 19]}$$

where β_1 = 0.85 if $f'_c < 4000$ psi
= 0.85 - 0.05[(f'_c - 4000)/1000] if $4000 < f'_c < 8000$ psi
= 0.65 if $f'_c > 8000$ psi

The amount of reinforcement provided ($\rho_{provided}$) in the design is:

$$\rho_{provided} = \frac{A_{FRP}}{b\,d} \quad \text{[Eq 20]}$$

The maximum reinforcement provided is limited to the following expression to rule out severe deflection problems due to the beam's difficulty in efficiently carrying the design moment. The limiting maximum reinforcement ratio (ρ_{max}), stated in ACI 10.3.3, is:

$$\rho_{max} = 0.75\,\rho_{bal} \quad \text{[Eq 21]}$$

ACI 10.5.1 requires a minimum reinforcement ratio limit to be provided. It is required for increasing the strength of concrete. Usually, the beam depth is increased to avoid surpassing this limit. If the depth can not be increased, doubly reinforced beams should be used. The minimum reinforcement (ρ_{min}) limit is given as:

$$\rho_{min} = 2.7 \frac{\sqrt{f'_c}}{f_y} \quad \text{[Eq 22]}$$

If $\rho_{min} < \rho < \rho_{max}$ then ρ provided in the design is acceptable.
If $\rho < \rho_{min}$ then provide ρ_{min} .
If $\rho > \rho_{max}$ then increase the section dimensions, and/or design the beam for a compression failure complying with ductility requirements.

To avoid brittle compression failure of concrete, all sections should be designed as under-reinforced, with c/d ratios less than the balanced condition. This approach allows the reinforcement to yield before the concrete fails in compression. The ductile yielding of the reinforcements causes the formation of cracks to give warning before failure.

Bond Strength and Development Length

The straight pull-out test is used to determine the bond quality of FRP rebars. The results of cantilever specimens are evaluated to design for appropriate embedment length of FRP rebars. The proper length is important to minimize bond slip, which enables the rebars to attain full anchorage without bond failure. Equilibrium conditions give the anchorage pulling force equal to the tensile force of the rebar cross section, as shown in Figure 5. This yields the following expressions (as given in section 5.5.1 of the CFC-92-142).

$$\mu \pi d_b l_d = \frac{\pi d_b^2}{4} f_t \qquad \text{[Eq 23]}$$

where μ = bond strength (psi)
d_b = rebar diameter (in.)
l_d = embedment length (in.)

From this equation, the bond strength (μ) can be derived as:

$$\mu = \frac{f_t d_b}{4 l_d} \qquad \text{[Eq 24]}$$

Using the ACI approach, the development length of rebars in tension is computed as a function of rebar size, yield strength, and concrete compressive strength. ACI 12.2.2 gives the development length (l_{db}) for steel rebar size #11 or smaller as:

$$l_{db} = 0.04 A_b \frac{f_y}{\sqrt{f'_c}} \qquad \text{[Eq 25]}$$

where A_b = area of rebar (in^2)

Modification of the development length equation to accommodate FRP rebar results in the expression, as given in equation (5-42) of the CFC-92-142:

$$l_{db} = 0.06 A_b \frac{f_y}{\sqrt{f'_c}} \qquad \text{[Eq 26]}$$

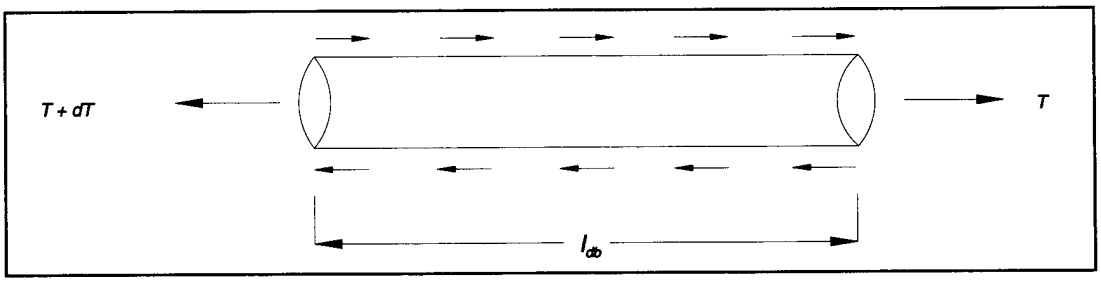

Figure 5. Bond anchorage.

The design methodologies presented above were used in the concrete bridge deck design documented in Chapter 4. The FRP concrete deck is designed in a procedure similar to the working stress design method of transversely reinforced concrete decks found in AASHTO* 1995. Analysis of the bridge is performed using HS 25 truck loading. This loading is a modification of AASHTO's HS 20 loading that proportionally factors the loads higher.

It should be noted that the equations presented above can be applied to one-way slab design even though they were developed in this study for beam design.

* AASHTO: American Association of State Highway and Transportation Officials.

4 Bridge Deck Design

Introduction

The new concrete deck of the replacement McKinleyville bridge has a span of 177 ft (three sections, 52 ft, 73 ft, and 52 ft) and a width of 29 ft-6 in. It consists of two lanes and is supported by six steel stringers at 5 ft spacing. The stringer size is W 33 x 130. Deck specifications are summarized in Table 1.

Details and Specifications

According to AASHTO 3.24.1.2 b, the span length (L) is the distance between the edges of the flanges plus half the stringer flange width. The flange width (b_f) is 11.5 in. for the W 30 x 130 section according to *AISC Manual of Steel Construction*

Table 1. Specifications for replacement McKinleyville Bridge.

Property	Symbol	Value
Avg. concrete compressive strength	f'_c	4500 psi
Allowable concrete stress	$f_c = 0.45\, f'_c$	2025 psi
Concrete weight	W_c	150 psf
Concrete modulus	$E_c = 57000\, (f'_c)^{½}$	3.82×10^6 psi
Wearing surface weight	W_s	25psf
Allowable FRP rebar stress	f_f	20000 psi
FRP rebar yield strength (#4 rebar)	f_y	85600 psi
FRP rebar modulus (#4 rebar)	E_{FRP}	7.2×10^6 psi
Top clear cover		1.5 in
Bottom clear cover		1.0 in
Stringer steel		Grade 50
Deck thickness	t_s	9 in
Stringer spacing	s	5 ft

(1980). Figure 6 shows an elevation view of the deck and stringers. The span length is:

$$L = s - \frac{b_f}{2}$$
$$= 60in - \frac{11.5in}{2} = 54.25\ in = 4.52\ ft \qquad \text{[Eq 27]}$$

The uniform dead load (W_{DL}) and dead load moment (M_{DL}) are computed by considering a continuous span with a moment of $M_{DL} = WL^2/10$. This equation incorporates a 0.8 factor for continuity on the simply supported case of $WL^2/8$, similar to the provision for live load given in AASHTO 3.24.3.1. Taking a 1 ft section with a uniform dead load, the load and moment per foot are calculated to be:

$$W_{DL} = t_s x W_c + W_s$$
$$= \frac{9in}{12in/ft} x 150psf + 25plf \qquad \text{[Eq 28]}$$
$$= 137.5\ plf$$

$$M_{DL} = \frac{(137.5plf)(4.52ft)^2}{10} \qquad \text{[Eq 29]}$$
$$= 281\ lb\text{-}ft$$
$$= 0.281\ kip\text{-}ft$$

The live load of the deck is designed for HS 25 truck loading. This loading is obtained by proportionately changing the weights for the standard truck and corresponding lane loads. AASHTO 3.8.2.1 equation (3-1) gives the impact allowance (I) as:

$$I = \frac{50}{s + 125} \quad \text{with a maximum of 30\%}$$
$$= \frac{50}{5ft + 125} = 0.38 > 0.3 \quad \text{no good} \qquad \text{[Eq 30]}$$
$$\text{use } I = 0.3$$

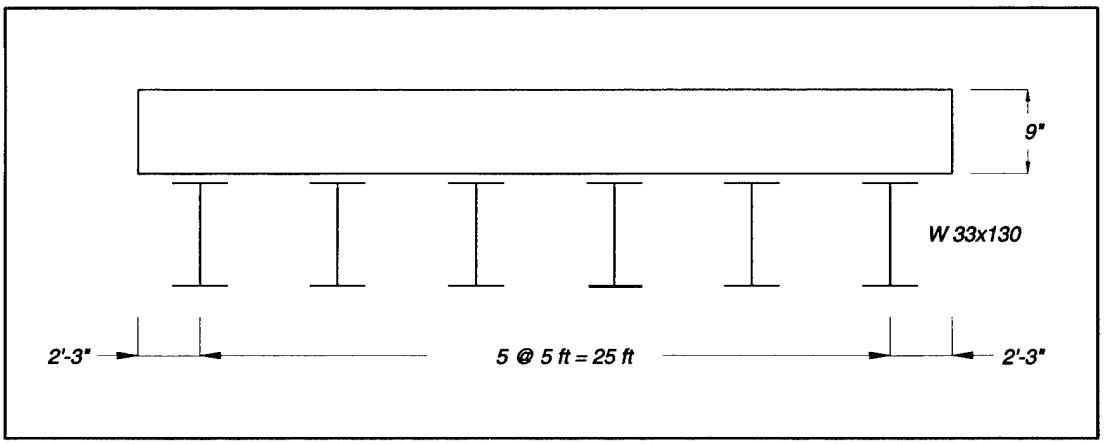

Figure 6. Slab dimensions.

The equation for the live load moment (M_{LL}) is also subjected to the 0.8 factor for continuity as per AASHTO 3.24.3.1. The load P is obtained by proportioning it to the standard truck load from AASHTO 3.7.6.

$$P_{25} = P_{20} x \frac{25}{20} = 16 lbs x \frac{25}{20} = 20 \ lbs \qquad \text{[Eq 31]}$$

The equation for M_{LL} includes impact and the continuity factor. The per foot live load moment is calculated to be:

$$\begin{aligned} M_{LL} &= (\frac{L+2}{32} P_{25} + \frac{L+2}{32} P_{25} x 0.3) \ x \ 0.8 \\ &= \frac{4.52 ft + 2}{32} (20 lbs) x 1.3 x 0.8 \\ &= 4.24 \ kip\text{-}ft \end{aligned} \qquad \text{[Eq 32]}$$

The service load design is performed with the total unfactored moment (M_T), which is given as the sum of the dead and live load moments.

$$\begin{aligned} M_T &= M_{DL} + M_{LL} \\ &= 0.281 + 4.24 = 4.52 \ kip\text{-}ft \end{aligned} \qquad \text{[Eq 33]}$$

The modular ratio, as stated in the design methodology, is used to convert between FRP and concrete properties:

$$\begin{aligned} n &= \frac{E_{FRP}}{E_c} \\ &= \frac{7.2 x 10^6 \ psi}{3.82 x 10^6 \ psi} = 1.88 \end{aligned} \qquad \text{[Eq 34]}$$

FRP transverse reinforcement is the main reinforcement provided in the bridge deck. Referring to Figure 7, the following information is obtained:

The top cover is: 1.5 in.
The bottom cover is: 1 in.

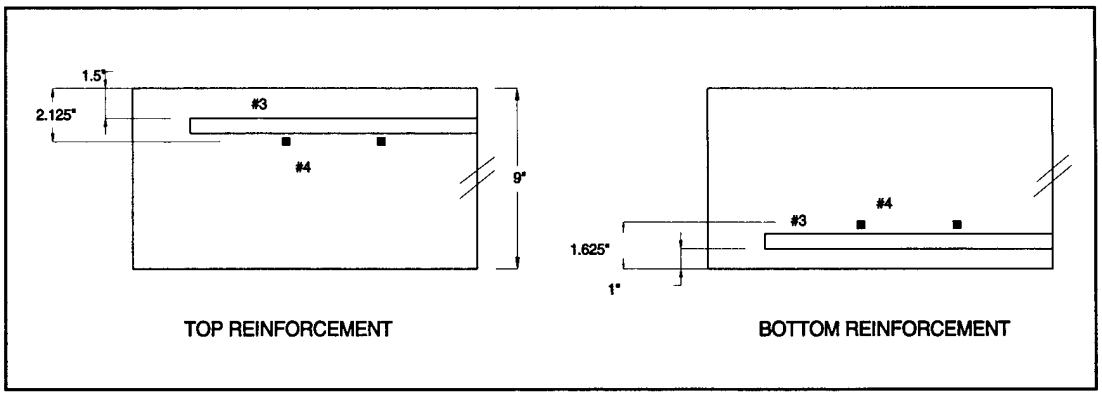

Figure 7. Reinforcement detail.

Diameters of rebar #3 and #4: 0.375 in and 0.5 in, respectively
Effective depth d at the top: 9 - (1.5 + 0.375 + 0.25) = 6.875 in.
Effective depth d at the bottom: 9 - (1 + 0.375 + 0.25) = 7.375 in.

CFC-92-142 section 6.1 gives the working stress design expressions. The variable "kd" is the distance from the top of concrete to the neutral axis, where "k" is a proportionate multiplier. The equation for calculating the area of FRP includes the conversion factor of 12,000 lb-in/kip-ft. Area of FRP for the top ($A_{FRP\ top}$) at midspan is calculated by:

$$k = \frac{n f_c}{n f_c + f_f} = \frac{1.88\,(2025\,psi)}{1.88\,(2025\,psi) + 20000\,psi} = 0.16 \qquad \text{[Eq 35]}$$

$$A_{FRP\ top} = \frac{M_T \times 12000}{f_f d(1 - k/3)} = \frac{4.52\,kip\text{-}ft \times 12000}{20000\,psi(6.875\,in)(1 - 0.16/3)} = 0.416\ in^2 \qquad \text{[Eq 36]}$$

Area of FRP for the bottom ($A_{FRP\ bottom}$) at midspan is calculated by:

$$A_{FRP\ bottom} = \frac{M_T \times 12000}{f_f d(1 - k/3)} = \frac{4.52\,kip\text{-}ft \times 12000}{20000\,psi(7.375\,in)(1 - 0.16/3)} = 0.39\ in^2 \qquad \text{[Eq 37]}$$

Therefore, provide #4 @ 6 in c/c, giving a FRP area of 0.39 in^2 for a 1 foot span. This applies to both the top and bottom midspan sections.

The maximum moment capacity can be determined from the rectangular stress distribution diagram shown in Figure 2 (Chapter 3). According to ACI 10.2.7.1, the variable "a" is determined by equilibrating the tensile force ($T = A_{FRP}\ f_y$) with the compressive force ($C = 0.85 f'_c ab$). The nominal moment capacity equation follows the form expressed in ACI 9.1, with $\phi = 0.9$ as the moment capacity factor and 12,000 lb-in/kip-ft as the conversion factor.

At midspan:

$$a = \frac{A_{FRP} f_y}{0.85 f'_c b} = \frac{(0.39\,in.^2)(85600\,psi)}{0.85\,(4500\,psi)(12\,in.)} = 0.727\ in. \qquad \text{[Eq 38]}$$

$$M_u = \phi A_{FRP} f_y (d - \frac{a}{2})$$
$$= 0.9(0.39 in^2)(85600 psi)(7.375 in - \frac{0.727 in}{2}) x \frac{1}{12000} \quad \text{[Eq 39]}$$
$$= 17.55 \ kip\text{-}ft$$

Over the stringers:

$$M_u = \phi A_{FRP} f_y (d - \frac{a}{2})$$
$$= 0.9(0.39 in^2)(85600 psi)(6.875 in - \frac{0.727 in}{2}) x \frac{1}{12000} \quad \text{[Eq 40]}$$
$$= 16.30 \ kip\text{-}ft$$

The moment carrying capacities at midspan of 17.55 kip-ft and over the stringer of 16.30 kip-ft are greater than the applied moment of 4.52 kip-ft, so there is adequate reinforcement.

A check for maximum reinforcement as stated in section 5.4 of CFC-92-142, with the maximum reinforcement given by ACI 10.3.3, is now required. β_1 relates the depth of the stress block to the distance between the compression surface and the neutral axis. The balanced reinforcement ratio (ρ_{bal}) is:

$$\beta_1 = 0.85 - 0.05 \frac{f'_c - 4000}{1000}$$
$$= 0.85 - 0.05 \frac{4500 psi - 4000}{1000} = 0.825$$
$$\rho_{bal} = \beta_1 \frac{0.85 f'_c}{f_y} x \frac{19500}{19500 + f_y} \quad \text{[Eq 41]}$$
$$= 0.825 (\frac{0.85 x 4500 psi}{85600 psi}) (\frac{19500}{19500 + 85600 psi}) = 0.007$$

The maximum reinforcement ratio (ρ_{max}) is found from the balanced reinforcement ratio as:

$$\rho_{max} = 0.75 \ \rho_{bal}$$
$$= 0.75 \ x \ 0.007 = 0.0052 \quad \text{[Eq 42]}$$

The amount of reinforcement provided ($\rho_{provided}$) must not exceed the maximum reinforcement ratio:

$$\rho_{provided} = \frac{A_{FRP}}{bd} = \frac{0.39 in^2}{12 in(6.875 in)} = 0.0047 < \rho_{max} \quad \text{[Eq 43]}$$

Because the amount of reinforcement provided (0.0047) is less than the maximum ratio of 0.0052, the design is valid. However, it should be noted that after the

completion of this study, a U.S./Canada task group comprising standards organizations, government agencies, and universities began a re-evaluation of this criterion. An over-reinforced section is being designed to revisit issues of compression failure and ductility responses (GangaRao 1996).

Distribution reinforcement near midspan is to be provided for the lateral distribution of the concentrated live load, and placed transverse to the main steel reinforcement. This reinforcement is designed according to AASHTO 3.24.10, equation (3-22). For main reinforcement perpendicular to traffic, the amount of distribution reinforcement is given as:

$$Percentage = \frac{220}{\sqrt{L}} \quad Maximum\ 67\%$$

$$= \frac{200}{\sqrt{4.52}} = 94.07\% > 67\% \qquad \text{[Eq 44]}$$

$$use\ 67\% \times 0.39 in^2 = 0.26\ in^2$$

When using #3 bars instead of #4 bars, a ratio can be applied to find the amount of #3 bars required to replace the #4 bars. CFC-92-142 Table 6.1 gives the yield strength of the #3 bar as 104 ksi and the yield strength of the #4 bar as 85.6 ksi. The amount of #3 bar required is:

$$A_{FRP\ required} = \frac{85.6}{104} x 0.26 in^2 = 0.21\ in^2 \qquad \text{[Eq 45]}$$

Thus, distribution reinforcements can be provided as #3 @ 6 in c/c to give an area of 0.22 in^2 over a 1 foot span.

Requirements for longitudinal reinforcement in the concrete deck near the piers is now examined. AASHTO 10.38.4.3 stipulates a minimum of 1 percent reinforcement in the negative moment regions of continuous spans. Using the information below, the amount of FRP reinforcement required can be calculated:

The top cover is: 1.5 in.
Diameter of #3 rebar is: 0.375 in.
The effective depth is: 9 - (1.5 + 0.1875) = 7.31 in.

$$A_{FRP\ required} = 0.01\, b\, t_s$$

$$= 0.01(12in)(9in) = 1.08\ in^2 \qquad \text{[Eq 46]}$$

Since longitudinal reinforcements of #3 stirrups are already provided for at 6 in c/c, this can be subtracted from the total FRP reinforcement required. After accounting for the existing reinforcement of 0.22 in^2 gives:

$$A_{FRP\ required} = 1.08 - 0.22 = 0.86\ in^2 \quad \text{[Eq 47]}$$

Thus, longitudinal reinforcement is provided as #6 @ 6 inches c/c in between #3 rebars. This yields 0.88 in^2 of reinforcement with a yield strength of 72 ksi for #6 bars.

To ensure that serviceability requirements are met, a check for maximum crack width (W_{max}) is determined according to CFC-92-142, section 5.2.2. For slabs, the value of β is 1.35. The effective concrete depth (d_c) is 2.125 in. The crack width equation is discussed in more detail in the design methodology section. The effective area of concrete surrounding the main reinforcement (A_c) and the crack width are:

$$A_c = \frac{2\,d_c\,b}{number\ of\ bars} = \frac{2(2.125\,in)(12\,in)}{2} = 25.5\ in^2 \quad \text{[Eq 48]}$$

$$W_{max} = 0.3\beta f_f \sqrt[3]{d_c A_c}\ x\ 10^{-3} = 0.3(1.35)(20\,ksi)\sqrt[3]{(2.125\,in)(25.5\,in^2)}\ x\ 10^{-3} = 0.031\ in \quad \text{[Eq 49]}$$

For FRP-reinforced concrete members, a crack width of this value is acceptable.

A check for the fatigue stresses in concrete requires checking the stress (σ) at the extreme fiber ends. Rearranging ACI 9.5.2.3 equation (9-8) gives $\sigma = My/I$. "M" is the moment, "y" is distance from center to the fiber ends (and is equal to $t_s/2$), and "I" is taken as the gross moment of inertia. This gives a stress value of:

$$\sigma = \frac{M}{b\frac{t_s^2}{6}} = \frac{4.52\,kip\text{-}ft\,x\,12000}{(12\,in)\frac{(9\,in)^2}{6}} = 335\ psi \quad \text{[Eq 50]}$$

This value is approximately 60% of the modulus of rupture. It should be noted that 50% of the modulus of rupture was found to be close to the endurance limit of

concrete under flexural fatigue. Thus, some flexural cracking may occur with time, but such cracks will have no effect on the capacity of the deck. ACI standards do not restrict the occurrence of cracking, but addresses crack spacing (as discussed above). This estimate is quite conservative, so designs falling above 50 percent are considered to be valid.

The moment capacity at the overhang is found by the following equation:

$$M = A_{FRP} f_f d\left(1 - \frac{k}{3}\right)$$
$$= 0.22\,in^2(20000\,psi)(7.375\,in)\left(1 - \frac{0.16}{3}\right) \quad \text{[Eq 51]}$$
$$= 2.56\ kip\text{-}ft$$

The moment due to the curb and overhang slab ($M_{overhang}$) is calculated by multiplying the weight of the curb and the overhang by their respective moment arms.

The area for the curb is approximated as 24 in by 21 in, as shown in Figure 8. The weight is found by multiplying the area by the weight of concrete as 0.150 ksf.

$$M = M_{curb} + M_{slab}$$
$$= (0.525\,kip)(1.375\,ft) + (0.150\,ksf)\frac{(2.25\,ft^2)}{2} \quad \text{[Eq 52]}$$
$$= 0.72 + 0.38 = 1.09\ kip\text{-}ft$$

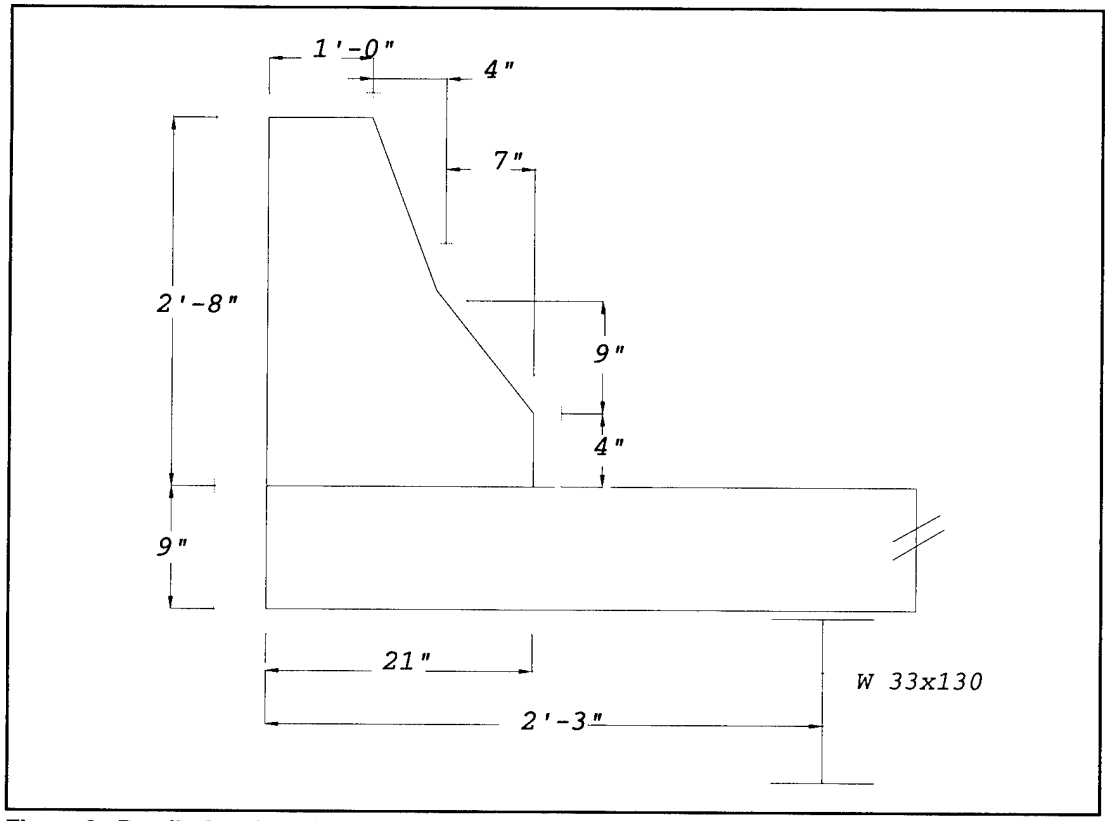

Figure 8. Detail of curb and overhang.

Since the moment due to the dead overhang loads of 1.09 kip-ft is less than the moment capacity at the overhang of 2.56 kip-ft, the design is suitable.

A check for the deflection of the slab is now performed. The total factored moment ($M_{factored}$), according to AASHTO Table 3.22.1A, is given as 1.3 (M_{DL}) + 1.3 (1.67) (M_{LL}) = 9.6 kip-ft. The equation for the cracked moment (M_{cr}) can be found in ACI 9.5.2.3 as:

$$M_{cr} = \frac{f_r I_g}{y} = f_r z$$
$$= 503.1\,psi\,(162\,in^3)$$
$$= 81502.2\,lb\text{-}in = 6.8\,kip\text{-}ft \qquad \text{[Eq 53]}$$

where

$$f_r = 7.5\sqrt{f'_c} = 7.5\sqrt{4500\,psi} = 503.1\ psi$$
$$z = \frac{bt_s^2}{6} = \frac{(12\,in)(9\,in)^2}{6} = 162\ in^3 \qquad \text{[Eq 54]}$$

Since the cracked moment of 6.8 kip-ft is less than the factored moment of 9.6 kip-ft, deflection is checked for the factored moment case. The distance "c" from the top of concrete to the cracked section can be found by equating the cracked concrete section with the FRP section. A_{FRP} of 0.39 in^2 is approximated to be 0.40 in^2.

$$\frac{bc^2}{2} = nA_{FRP}(d-c)$$
$$\frac{12c^2}{2} = 1.88(0.4)(7.375-c)$$
$$6c^2 = 0.752(7.375-c) \qquad \text{[Eq 55]}$$
$$7.98c^2 + c - 7.375 = 0$$
$$\text{solving for } c = 0.9\ in$$

The gross, cracked, and effective moment of inertias can be found in the design methodology section as:

$$I_g = \frac{bt_s^3}{12} = \frac{(12\,in)(9\,in)^3}{12} = 729\ in^4 \qquad \text{[Eq 56]}$$

$$I_{cr} = \frac{bc^3}{3} + nA_{FRP}(d-c)^2$$
$$= \frac{(12\,in)(0.9\,in)^3}{3} + 1.88(0.4\,in^2)(7.375\,in - 0.9\,in)^2 \qquad \text{[Eq 57]}$$
$$= 34.44\ in^4$$

$$I_e = I_{cr} + \left(\frac{M_{cr}}{M_{factored}}\right)^3 (I_g - I_{cr})$$
$$= 34.44\,in^4 + \left(\frac{6.8\,kip\text{-}ft}{9.6\,kip\text{-}ft}\right)^3 (729\,in^4 - 34.44\,in^4) \quad \text{[Eq 58]}$$
$$= 281.28\ in^4$$

The deflection (Δ) is then calculated using a length (l) of 0.8 x 60 = 48 in. The 0.8 factor is used to account for continuity of the span and the conversion factor of 12,000 lb-in/kip-ft is applied. The factored dead load moment (M_{DL}) = 1.3 (0.281 kip-ft) and live load moment (M_{LL}) = 1.3 (1.7) (4.24 kip-ft) are used in the following equation.

$$\Delta = \frac{5}{48}\frac{M_{DL}\,l^2}{EI_e} + \frac{M_{LL}}{12}\frac{l^2}{EI_e}$$
$$= \left(\frac{5}{48} x 0.361 x 48^2 + \frac{9.2}{12} x 48^2\right) \frac{12000}{3.82x10^6 \times 281.28} \quad \text{[Eq 59]}$$
$$= 0.022\ in$$

This value is less than length/1000 = 0.06 in., as required by AASHTO 8.9.3.1 as well as length/360 = 0.15 in., as required by ACI. Therefore, the deflection is acceptable.

The following deflection check is based upon the modified moment of inertia (I_m) for FRP-reinforced concrete members instead of steel-reinforced members. The design methodology equation gives I_m for the case of a concentrated load at the center and for a uniformly distributed load, respectively, by:

$$I_m = \frac{54\,I_{cr}\,I_e}{16\,I_{cr} + 38\,I_e} \quad \text{[Eq 60]}$$
$$= \frac{54(34.44)(281.28)}{16(34.44) + 38(281.28)} = 46.54\ in^4$$

and

$$I_m = \frac{240\,I_{cr}\,I_e}{39\,I_{cr} + 201\,I_e} \quad \text{[Eq 61]}$$
$$= \frac{240(34.44)(281.28)}{39(34.44) + 201(281.28)} = 40.17\ in^4$$

The deflection, as calculated with the modified moment of inertia, is given by:

$$\Delta = \frac{l^2}{12E_c}\left(\frac{M_{DL}}{4x40.17} + \frac{M_{LL}}{46.54}\right)$$
$$= \frac{48^2}{12x\,3.82x10^6}\left(\frac{0.361}{4x40.17} + \frac{9.2}{46.54}\right) x\ 12000 \qquad \text{[Eq 62]}$$
$$= 0.12\ in$$

The value of 0.12 in. is not less than the AASHTO 8.9.3.1 requirement of l/1000 = 0.06 in, but it is less than the ACI requirement of l/360 = 0.15 in. Deflections are required to satisfy the service load moments, not the factored moments. Recalculating this value for unfactored moments gives a value of 0.056 in., which satisfies the AASHTO requirement.

In this slab design, shear connections are designed using shear stud connectors of 7/8 in diameter (d) and 5 in height (h). The h/d ratio of 5.7 satisfies the AASHTO 10.38.5.1.1 requirement that welded studs be greater than or equal to 4. The AASHTO 10.38.5.1.2 equation (10-66) specification for ultimate strength of welded studs is used to determine the allowable load per stud (S_u). The factor of 1/1000 is a conversion factor from psi to ksi.

$$S_u = 0.4\ d^2\sqrt{f'_c E_c}$$
$$= 0.4\,x(0.875in)^2\sqrt{(4500psi)(3.82x10^6psi)}\ \ x\left(\frac{1}{1000}\right) \qquad \text{[Eq 63]}$$
$$= 40.17\ kips\ per\ stud$$

Taking α = 7.85 ksi for 2,000,000 cycles of load in the AASHTO 10.38.5.1 specification, the load range per shear connector (Z_r) is found from equation (10-59) as:

$$Z_r = \alpha\, d^2$$
$$= 7.85ksi(0.875in)^2 = 6.01\ kips\ per\ stud \qquad \text{[Eq 64]}$$

The shear connector strength requirement is performed according to AASHTO 10.38.5.1.2 equations (10-61) and (10-62). A_s is the cross-sectional area of the W 30 x 130 stringer while f_y is the strength of the shear studs. The force in the slab (P) is given as the smaller of the following two values:

$$P_1 = A_s f_y$$
$$= 38.3in^2(36ksi) = 1378.8\ kips \quad (governs) \qquad \text{[Eq 65]}$$

$$P_2 = 0.85f'_c bt_s$$
$$= 0.85(4.5ksi)(60in)(9in) = 2065.5\ kips \qquad \text{[Eq 66]}$$

The number of studs (N) required between the middle of the central span and the pier is given by AASHTO 10.38.5.1.2 equation (10-60) as:

$$N = \frac{P}{\phi S_u} = \frac{1378.8\,kips}{0.85(40.17\,kips/stud)} = 40.38 \approx 41\ studs \quad \text{[Eq 67]}$$

The shear connector spacing required for fatigue behavior needs to be satisfied. At the internal supports, the shear range for the live load has been computed by considering the midspan to be simply supported. Appendix A in AASHTO gives the live load shear for an HS 20 (MS-18) loading as 63.1 kips for a 75 ft span bridge. This is a conservative value, considering the longest span in this bridge is 73 ft. Factoring this for an HS 25 loading gives 63.1 x 25/20 = 78.9 kips for the live load shear. "Q" is the static moment about the neutral axis, as given in AASHTO 10.38.5.1.1. The shear per inch (S_r) is calculated by:

$$S_r = \frac{V_r Q}{I} = \frac{(78.9\,kips)(354.2\,in^3)}{40301\,in^4} = 0.69\ kips/in \quad \text{[Eq 68]}$$

where I = composite moment of inertia (slab and stringer) = 40301 in.^{4} and

$$Q = t_s x \frac{t_s}{2} x s = 9\ in\ (\frac{9\ in}{2})(\frac{60\ in}{6.86\ in}) = 354.2\ in^3 \quad \text{[Eq 69]}$$

The spacing (S) required for 2 studs is:

$$S = \frac{2 Z_r}{S_r} = \frac{2(6.01\,kips)}{0.69\,kips/in} = 17.42\ in \quad \text{[Eq 70]}$$

Therefore, studs of 2-7/8 in. diameter at 17 in. c/c (each 5 in. in height) must be provided.

Modifications for Using Rebars From Marshall Industries

Due to the sizes of non-coated rebar available from Marshall Industries it was necessary to substitute #4 bar where #3 had been specified, and #5 rebar where #6 had previously been indicated.

With a top cover of 1.5 in, the effective depth becomes 9 - 2.25 = 6.75 in. The area of FRP rebars required can be determined to be:

$$Area_{FRP} = \frac{M \times 12000\,kip\text{-}ft}{f_f d(1 - \frac{k}{3})} = \frac{4.52\,kip\text{-}ft \times 12000}{20000\,psi(6.75\,in)(1 - \frac{0.16}{3})} = 0.424\ in^2 \quad \text{[Eq 71]}$$

Therefore, #5 rebar, spaced 6 in c/c, provides an area of 0.62 in^2.

The bottom cover is 1 in, so the effective depth becomes 9 - 1.75 = 7.25 in. The amount of reinforcement provided at the bottom of the midspan section between stirrups is:

$$Area_{FRP} = \frac{M \times 12000}{f_f d(1 - \frac{k}{3})} = \frac{4.52\,kip\text{-}ft \times 12000}{20000\,psi(7.25\,in)(1 - \frac{0.16}{3})} = 0.395\ in^2 \quad \text{[Eq 72]}$$

Bottom reinforcement should be provided as #4 @ 6 in c/c to give an area of 0.39 in^2.

For the concrete deck, AASHTO requires a minimum of 1 percent longitudinal reinforcement. This gives:

$$A_{FRP\ required} = 0.01\,bt_s = 0.01(12\,in)(9\,in) = 1.08\ in^2 \quad \text{[Eq 73]}$$

Since #4 @ 6 in c/c is already used for longitudinal reinforcement, the final FRP requirement should take into consideration the existing reinforcement of 0.39 in^2.

$$A_{FRP\ required} = 1.08 - 0.39 = 0.69\ in^2 \quad \text{[Eq 74]}$$

Providing #6 @ 6 in c/c gives an area of 0.88 in^2, which is adequate.

Provisions for the basic development length are given in ACI 12.2.2. For #4 bar with f_f = 80000 psi and f'_c = 4500 psi, the equation is:

$$l_{db} = 0.04\,A_b \frac{f_y}{\sqrt{f'_c}} = 0.04(0.19\,in^2)\frac{80000\,psi}{\sqrt{4500\,psi}} = 9.06\ in \quad \text{[Eq 75]}$$

Modification of 1.3 for top reinforcement and 1.5 for epoxy coated reinforcement exist in ACI 12.2.4.1 and 12.2.4.3, respectively. Modifying the development length gives a value of:

$$l_{db} = (9.06in)(1.3)(1.5) = 17.67 \approx 18\ in \quad \text{[Eq 76]}$$

For the FRP rebars, the development length is found in GangaRao and Faza (1992) section 5.5.2.2 as:

$$l_{db} = 0.06 A_b \frac{f_y}{\sqrt{f'_c}} = 0.06(0.19in^2)\frac{80000psi}{\sqrt{4500psi}} = 13.59\ in \quad \text{[Eq 77]}$$

The modification factor for the top reinforcement is valid here, but the epoxy-coated reinforcement factor already has been accounted for by the FRP rebars. The development length comes to:

$$l_{db} = 13.59in(1.3) = 17.67 \approx 18\ in \quad \text{[Eq 78]}$$

For rebars with f_y = 60,000 psi, the basic development length for hooked bars is given in ACI 12.5 as:

$$l_{db} = 1200 \frac{d_b}{\sqrt{f'_c}} = 1200\,x\frac{0.5}{\sqrt{4500}} = 8.94\ in \quad \text{[Eq 79]}$$

ACI modifications for rebars with f_y > 80,000 psi is 80,000/60,000 = 1.33, and for epoxy-coated rebars the figure is 1.5. The final value for the development length is:

$$l_{db} = 8.94in(1.33)(1.5) = 17.84 \approx 18\ in \quad \text{[Eq 80]}$$

According to Ehsani, Sandatmanesh, and Tao (1996), rebars with a f_y = 75,000 psi have a development length given by:

$$l_{db} = 1824 \frac{d_b}{\sqrt{f'_c}} = 1824\,x\frac{0.5}{\sqrt{4500}} = 13.59\ in \quad \text{[Eq 81]}$$

Modifications for rebars with f_y = 80,000 psi is 80,000/75,000 = 1.07, while the epoxy-coated factor is not applicable. This gives a final value of:

$$l_{db} = 13.59in(1.07) = 14.49 \approx 14.5\ in \quad \text{[Eq 82]}$$

This value is lower than the previous calculations so a conservative development length of 18 in. should be provided.

The equation provided by ACI 10.6.4 for the allowable crack width using steel reinforcement is:

$$W_{max} = 0.076 \beta f_f \sqrt[3]{d_c A} \times 10^{-3} \quad inches \qquad \text{[Eq 83]}$$

This equation can be modified for FRP-reinforced concrete members. Using E_{FRP} = 7.2 x 10^6 psi as an upper bound and E_s = 29.5 x 10^6 psi, the ratio of E_s / E_{FRP} = 4.0. Using this, the maximum crack width equation can be modified to be:

$$W_{max} = 0.3 \beta f_f \sqrt[3]{d_c A} \times 10^{-3} \quad inches \qquad \text{[Eq 84]}$$

For a lower bound estimate of the crack width, use E_{FRP} = 6.0 x 10^6 psi to obtain a ratio of E_s / E_{FRP} = 4.92. The modified equation becomes:

$$W_{max} = 0.37 \beta f_f \sqrt[3]{d_c A} \times 10^{-3} \quad inches \qquad \text{[Eq 85]}$$

The above two equations are valid for design stress levels in FRP rebars equal to 20 ksi. They can be found in GangaRao and Faza (1992), section 5.2.2. The upper bound equation yields a crack width of 0.031 in. while the lower bound equation gives a crack width of 0.038 in.

5 Rebar Placement and Concrete Deck Construction

Rebar Placement

The West Virginia University–Constructed Facilities Center performed tensile testing of FRP bars supplied by the FRP manufacturers before using those bars for the McKinleyville bridge construction. The ultimate tensile strength and Young's modulus (stiffness) of FRP bars were established as a part of the researcher's quality control program. The bars were approved for placement in the bridge deck by the Materials Division of WVDOT–DOH after testing and making sure that minimum strength and stiffness results are attained.

Epoxy-coated steel chairs (1 in.), for bottom cover, were spaced 4 ft apart to support main reinforcement in the bridge at the bottom. In addition, 7 in. high chairs were placed between 1 in. chairs to support the top bars used for temperature and shrinkage control. The chair spacing was based on limiting bar deflections under construction loads such as concreting equipment and crew.

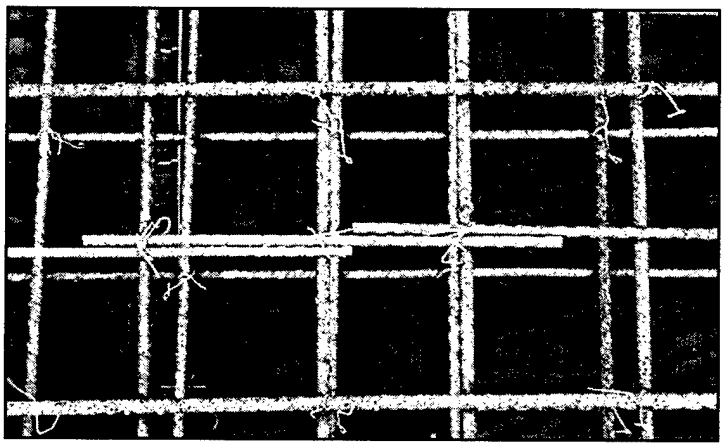

Figure 9. Sand-coated FRP rebar mesh tied in place.

There was a general concern about the possible flotation of FRP bars while casting concrete. The FRP mesh was tied down to the formwork at 4 ft intervals in both the transverse and longitudinal directions to maintain adequate cover (Figures 9 and 10).

Figure 10. Non-coated FRP rebar mesh tied in place.

The FRP bars withstood typical onsite handling during concreting. The construction crew was able to handle the FRP bars the same way they handle steel, but with one important distinction: FRP rebars are only one-quarter to one-fifth the weight of steel rebars of the same grade and length. Therefore, laborers could (1) carry lighter loads from the rebar-cutting area to the deck with no loss of productivity or (2) they could carry more bars at a time, thereby reducing the number of trips required between the cutting area and the deck. The deck construction process in this demonstration was not specifically organized to document the impact on labor of using lighter reinforcement materials, but the lighter weight has some obvious positive implications for construction productivity. (See Chapter 6.)

Casting the Concrete Deck

The concrete deck was cast in two pours. The first part was about 10 ft from the north abutment to about 10 ft from the south abutment, corresponding nearly to the inflection points of the superstructure near abutments. The first pour was in the evening hours (7:30 p.m. to 2:30 a.m.) on 1–2 August 1996. Those hours were selected to minimize shrinkage- and temperature-associated cracks. The concrete was supplied by a local vendor. A slump of 3.5–4.0 in. was maintained throughout the deck casting. The second pour—casting of remaining portions of bridge deck, integral abutment, and approach slab—started at 7:00 a.m. and was concluded at 10:00 a.m. on 2 August 1996. The concrete was vibrated for about 9–10 seconds at each place and at a spacing of about 20 in. The ambient temperature ranged between 75 °F–80 °F during concreting.

Curing the Concrete

The concrete deck, including abutments and approach slabs, was cured for 14 days covered with wet burlap and plastic. Constant wetting of concrete surfaces was ensured by continuously flowing water over them.

6 Construction Productivity and Cost Issues

As noted in Chapter 5, FRP composite rebar is handled and tied essentially in the same manner as conventional steel rebar. Therefore, construction personnel do not need any special training to handle and install FRP composite rebar. One difference between FRP rebar and steel rebar, however, is that the thermoset resins used in FRP rebar do not allow the finished product to be bent in the field. Manufacturers offer standard bends, and custom bends can be ordered. Marshall Industries—one of the manufacturers who provided FRP rebar for this project—is currently working on a portable system that could travel to a construction site and produce the the specific bends necessary for the job. However, at the time of publication of this report, this system was not yet available.

Construction productivity improvements resulting from this technology relate to the lower density of FRP composites as compared to the mild steel used in conventional rebar. Marshall Industries advertises its FRP composite rebar, called C-BAR™, to be only 25 percent the weight of steel (Marshall Industries 1996). Similarly, the professional experience of WVU-CFC researchers indicates that FRP composites may range to as little as 20 percent the weight of mild steel rebars of the same dimensions. Therefore, it is reasonable to infer that a laborer can carry FRP composite rebar with one-quarter of the effort it takes to move the same amount of conventional steel rebar. Stated another way, a laborer should be able to carry about four times the number of FRP composite rebars on a single trip without experiencing additional physical strain. Regardless of how the productivity impact is accounted for (e.g., fewer laborers required onsite, faster throughput times for transporting and installing rebar, reduced physical strain on laborers), it is clear that slashing rebar weight by 75 percent would have a positive impact on construction productivity for reinforced concrete structures.

Cost comparisons between FRP composite and mild steel rebars are related to several factors. First is the cost per lineal foot. Current rebar prices range as follows:

- mild steel (#4) = $0.18/ft
- epoxy-coated mild steel (#4) = $0.35

- FRP rebar (#4) from International Grating = $0.50 – $0.68
- FRP rebar (#4) from Marshall Industries = $0.60 – $0.64.

Note that the steel rebar prices may be subject to regional variations, and they may change according to quantity purchased. The price range shown for FRP rebar reflects differences according to quantity purchased.

FRP composite rebar costs should be compared to the cost of epoxy-coated steel because both of these materials are intended for use in corrosive environments. Another cost factor is the size and number of rebars necessary to accomplish the required reinforcement. Because FRP composite rebars have a higher ultimate tensile strength than steel, it can be utilized with a higher working stress, thus improving the efficiency of the rebar and reducing the total material cost compared to epoxy-coated steel. However, until more is understood about the long-term durability of FRP rebar, conservative working stresses must be applied to designs. As noted in Chapter 4, the allowable FRP rebar stress for the bridge deck design is 20,000 psi, while the tensile yield strength for #4 FRP rebar is 85,600 psi. Allowable FRP rebar stress should be kept at less than 25 percent of the tensile yield strength until more is known about the creep, creep rupture, and fatigue behavior of FRP rebar.

Life-cycle costs analyses comparing FRP rebars to steel rebars cannot be conducted with confidence until more is known about the material's long-term durability. However, experience with FRP composite materials in other applications such as underground storage tanks, chemical plants, aerospace, and marine applications shows that FRP composites can be very durable in harsh environments. However, the choice of resin system in the composite can affect the long-term durability of FRP composites depending on the specific nature of the intended environment. Previous WVU–CFC research on FRP rebars with different resins systems indicates that reductions can occur in tensile strength and tensile stiffness when the material is subjected to accelerated aging tests in various harsh environments (GangaRao et al. 1996; Altizer et al. 1996). Based on the results of that testing, urethane modified vinyl ester resins were specified for the rebars used in the McKinleyville replacement bridge. However, the WVU–CFC results are preliminary, and further testing is necessary to fully understand the long-term durability of FRP composite rebars embedded in concrete. With appropriate choices of glass reinforcing fibers and resins, FRP rebar should exhibit good long-term durability (i.e., on the order of 30 years or more).

7 Conclusions, Recommendations, and Commercialization

Conclusions

The purpose of this work was to demonstrate the advantages of using FRP composite rebars in a full-scale reinforced concrete bridge deck, with attention to improving construction productivity and long-term system durability (i.e., corrosion resistance).

From the results of this project, it is concluded that the use of FRP rebars can improve construction productivity for reinforced concrete bridge decks. The FRP reinforcement system designed for this project was handled, placed, and tied using the conventional procedures required for installing standard steel rebar. No new training was needed for the construction contractors, and no modifications of concrete material or casting procedures were required. The lower weight of the FRP rebar—only 20 to 25 percent the weight of mild steel—allowed easier handling by the construction crew during installation. It can be concluded that this weight differential will enhance productivity related to the handling and carrying of rebar at the worksite.

Based on current purchase prices for mild steel, epoxy-coated steel, and FRP composite rebar, FRP is more expensive per lineal foot than mild steel and epoxy-coated steel. FRP #4 rebar currently costs about $0.50 per lineal foot whereas epoxy-coated mild steel rebar of the same grade costs $0.35 per lineal foot. Any potential cost benefits from using FRP instead of mild steel or epoxy-coated steel would take the form of longer bridge deck life cycle. No reliable life-cycle cost analysis can be conducted until the in-place durability of the FRP rebar has been monitored over the long term. Therefore, life-cycle cost conclusions cannot be drawn at this time.

Conclusions about the durability of FRP rebar must be based on long-term monitoring and data collection. During construction, the bridge deck was fully outfitted with strain gages and temperature sensors. WVU–CFC will monitor the long-term performance of the replacement McKinleyville Bridge deck beyond the

duration of this CPAR project, and the researchers will develop life-cycle cost data as part of the ongoing WVU–CFC research program.

Recommendations

Based on the short-term results of this project, FRP rebars can be recommended for use as a concrete reinforcement in similar applications.

Experience with FRP composite materials in other applications such as underground storage tanks, chemical plants, aerospace, and marine applications shows that FRP composites can be very durable in harsh environments. Therefore, with two caveats, FRP can be recommended for use in corrosive environments such as bridge decks and waterfront uses:

- As discussed in Chapter 6, the type of resin system used in the composite can have a significant impact on the long-term durability of FRP composites, depending on the specific nature of the intended environment. Therefore, before specifying a particular product, it is strongly recommended that engineers and specifiers thoroughly review the literature for the most current findings on resin performance in unique or demanding chemical environments.
- Because the creep behavior of FRP rebar is not fully understood at this time, it is recommended that FRP rebar use should be limited to low dead load applications.

To expand the potential applicability of FRP composite rebars, it is recommended that FRP rebar material parameters such as creep and fatigue also be monitored and studied.

Technology Transfer and Commercialization Plan

The two FRP rebar manufacturers that participated in this demonstration, Marshall Industries Composites and International Grating, work on a continual basis with WVU–CFC and other universities to develop FRP composite rebars as well as marketing strategies for these rebars. Developmental work is further advanced by other companies such as resin producers (Reichhold, Inc., and Ashland Chemicals, Inc.) and fiber producers (Owens-Corning and PPG). The FRP rebar manufacturers have been identifying mechanical and thermal properties of these rebars under varying environmental conditions. Resin characteristics have been

modified to enhance the durability of the product under various environmental conditions, including sustained loads.

Marshall Industries and International Grating also are aggressively promoting independent research by supplying FRP rebars at no cost to researchers at leading universities, where the products are evaluated for thermal-mechanical response to various conditions. The companies also have supplied FRP composite rebars at no cost for use in field applications, as they were supplied in support of this CPAR project.

Leading industry standards organizations are developing specifications and standards for using FRP rebar in reinforced concrete. American Concrete Institute (ACI) Committee 440, "Fiber Reinforced Plastic Reinforcement," is developing design guidance for FRP reinforcement. Draft guidance has been developed and is now being reviewed for acceptance. Also, the American Society for Testing and Materials (ASTM) Task Group D20.18.01, "FRP Composites for Concrete Reinforcement," is working to standardize terminology, material properties, classifications, and test methods. Several draft documents have been developed by this committee for balloting and approval by the main committee. ASTM Task Group D20.18.01 works closely with ACI Committee 440 to ensure consensus on important material parameters.

WVU–CFC has organized the U.S./Canada Joint Study Group on Concrete Members Reinforced With FRP Rebars, a panel dedicated to information exchange and cooperation in the development of standards and design guidance. Members include representatives of U.S. and Canadian code organizations, government agencies, and universities.

References

Altizer, S.D., P.V. Vijay, H.V.S. Gangarao, N. Douglass, and R. Pauer, "Thermoset Polymer Performance Under Harsh Environments to Evaluate Glass Composite Rebars for Infrastructure Applications," published at the Composite Institute's 51st Annual Conference and Exposition, Cincinnati, OH, 5–7 February 1996, pp 3C-1 to 3C-10.

Building Code Requirements for Reinforced Concrete, ACI 318-89, revised 1992 (American Concrete Institute [ACI], Detroit, MI, 1992).

Ehsani, M.R., H. Sandatmanesh, and S. Tao, "Bond Behavior and Design Recommendations for Fiberglass Reinforcing Bars," *Proceedings of the First International Congress on Composites Infrastructure*, Tucson, AZ, January 1996, pp 466-477.

GangaRao, Hota V.S., *Proposed Design of Concrete Members Reinforced With FRP Rebars*, presented to U.S./Canada Joint Study Group on Concrete Members Reinforced With FRP Rebars, 10 August 1996, Montreal, Quebec (West Virginia University–Constructed Facilities Center [WVU–CFC], Morgantown, WV).

GangaRao, Hota V.S., N. Douglass, R. Pauer, S.D. Altizer, and P.V. Vijay, "Thermoset Polymer Performance Under Harsh Environments to Evaluate Glass Composite Rebars for Infrastructure Applications," presented at the 1996 Spring Convention of the American Concrete Institute, 14–19 March 1996, Denver, CO.

GangaRao, Hota V.S., and Salem S. Faza, *Bending and Bond Behavior and Design of Concrete Beams Reinforced With Fiber Reinforced Plastic Rebars*, CFC-92-142 (WVU–CFC, Morgantown, WV, 1992).

"Introducing Marshall Industries C-BAR (TM) Reinforcing Rod," product literature (Marshall Industries Composites, Lima, OH, 1996).

Manual of Steel Construction, 8th ed. (American Institute of Steel Construction [AISC], Inc., Chicago, IL 1980).

Standard Specifications for Highway Bridges, 15th ed. (American Association of State Highway and Transportation Officials [AASHTO], Washington, DC, 1995).

Watstein, D., and B. Bresler, *Reinforced Concrete Engineering*, vol 1 (John Wiley & Sons, 1972).

USACERL DISTRIBUTION

Chief of Engineers
ATTN: CEHEC-IM-LH (2)
ATTN: CEHEC-IM-LP (2)
ATTN: CECC-R
ATTN: CECW
ATTN: CECW-OM
ATTN: CECW-P
ATTN: CECW-PR
ATTN: CERD-L

CECPW 22310-3862
ATTN: CECPW-E
ATTN: CECPW-FT
ATTN: CECPW-ZC

US Army Engr District
ATTN: Library (40)

US Army Engr Division
ATTN: Library (11)

Defense Tech Info Center 22304
ATTN: DTIC-O (2)

66
12/95